Journal of Luminescence 131 (2011) 2711–2715

Contents lists available at ScienceDirect

Journal of Luminescence

journal homepage: www.elsevier.com/locate/jlumin

OSL, RL and TL characterization of rare-earth ion doped K_2YF_5: Application in dosimetry

J. Marcazzó [a,b,c,*], E. Cruz-Zaragoza [c], Vu Xuan Quang [d], N.M. Khaidukov [e], M. Santiago [a,b]

[a] Instituto de Física Arroyo Seco, Universidad Nacional del Centro de la Provincia de Buenos Aires (UNICEN), Pinto 399, 7000 Tandil, Argentina
[b] Consejo Nacional de Investigaciones Científicas y Técnicas (CONICET), Rivadavia 1917, 1033 Buenos Aires, Argentina
[c] Instituto de Ciencias Nucleares, Universidad Nacional Autónoma de México, A.P. 70-543, 04510 México D.F., Mexico
[d] Institute of Materials Science, 18 Hoang Quoc Viet Rd., Hanoi, Viet Nam
[e] Institute of General and Inorganic Chemistry, RAS, 31 Leninskii Prospekt, 119991 Moscow, Russia

ARTICLE INFO

Article history:
Received 9 February 2011
Received in revised form
1 July 2011
Accepted 4 July 2011
Available online 13 July 2011

Keywords:
Fluorides
Optically stimulated luminescence
Radioluminescence

ABSTRACT

Optically stimulated luminescence (OSL) properties of K_2YF_5 crystals singly doped with different concentrations of Tb^{3+} ions and doubly doped with Tb^{3+} and Ce^{3+} or Tb^{3+} and Dy^{3+} have been investigated for the first time. Radioluminescence spectra and OSL efficiency for stimulation with different wavelengths of light have been analyzed for each compound. Also, dosimetric characteristics of the most efficient composition, namely K_2YF_5:1 at.% Tb^{3+}, have been studied. Finally, the OSL signal peculiarities for K_2YF_5:1 at.% Tb^{3+} have been compared to those of a commercial Al_2O_3:C dosimeter.

1. Introduction

Optically stimulated luminescence (OSL) is a good alternative to thermostimulated luminescence (TL) in radiation dosimetry due to several advantages [1]. One of such advantages is the fact that the stimulation method is completely optical, which makes it unnecessary to use a heating system for stimulating irradiated samples. For the same reason no thermal quenching occurs and more robust plastic encased OSL dosimeters can be easily manufactured. Moreover, high sensitivity of OSL allows multiple readings because it is not necessary to stimulate all of the trapped charges and the readout process can be made very fast by increasing the stimulating light intensity [1]. At present, C-doped alumina (Al_2O_3:C) could be considered as the standard material for OSL in practical dosimetry [2]. Recently it has been shown that sintered BeO could also become a promising OSL material for dosimetric purposes when taking into account its excellent tissue-equivalence and high efficiency [3,4].

In the context of the search for new dosimetric materials, doped potassium yttrium fluorides synthesized by the hydrothermal technique have shown to be efficient thermoluminescence (TL) and radioluminescence (RL) detectors [5–14]. Recently, the feasibility of employing these type of compounds as OSL dosimeters has also been demonstrated. In particular, the OSL properties of $K_2YF_5:Pr^{3+}$ under green stimulation have been studied and a very acceptable OSL response and good dosimetric properties have been found for this composition [15]. The efficient OSL emission of $K_2YF_5:Pr^{3+}$ is dominated by a characteristic luminescence band caused by the $^3P_0-{}^3H_4$ Pr^{3+} transition at 480 nm. Regretfully, the optical filters, which prevent the green stimulation light from reaching the light detector, also cut part of the OSL emission in this compound by reducing the overall efficiency for dosimetry. For this reason, optically active rare-earth ions showing characteristic emission at shorter wavelength could be better suited for doping K_2YF_5 than Pr^{3+}. In this context, there exists evidence that Tb^{3+} could meet this requirement. In fact, it has characteristic emission bands around 400 nm and also has shown to be an efficient activator when doped in different hosts [16,17,19].

In this work OSL properties of K_2YF_5 crystals singly doped with different concentrations of Tb^{3+} ions and doubly doped with Tb^{3+} and Ce^{3+} or Tb^{3+} and Dy^{3+} have been studied. Besides, the OSL efficiency of the investigated compounds has been compared to that of $K_2YF_5:Pr^{3+}$ crystals and a commercial Al_2O_3:C dosimeter. Finally, the dosimetric characteristics of the most efficient samples have been analyzed.

2. Experimental

Various compositions for K_2YF_5 singly doped with different concentrations of Tb^{3+} ions and doubly doped with Tb^{3+} and Ce^{3+} or Tb^{3+} and Dy^{3+} were synthesized with the hydrothermal

* Corresponding author at: Instituto de Física Arroyo Seco, Universidad Nacional del Centro de la Provincia de Buenos Aires (UNICEN), Pinto 399, 7000 Tandil, Argentina.
E-mail address: jmarcass@exa.unicen.edu.ar (J. Marcazzó).

0022-2313/$ - see front matter © 2011 Elsevier B.V. All rights reserved.
doi:10.1016/j.jlumin.2011.07.006

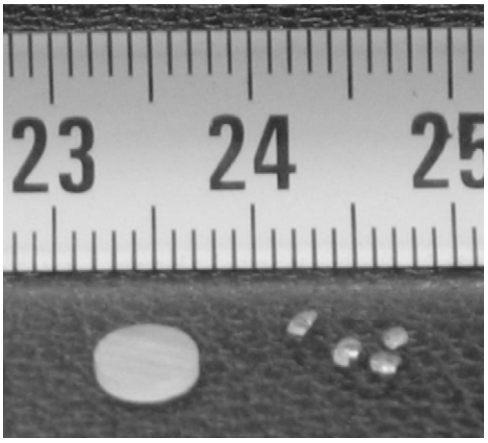

Fig. 1. Picture of the crystals employed in this work: a commercial Al_2O_3:C disc by Landauer Inc. (left) and rare-earth doped K_2YF_5 platelets, as grown by the hydrothermal technique (right).

technique [20]. Crystals of these fluoride compositions up to 1 cm^3 in size were grown by a direct temperature-gradient method as a result of the reaction of potassium fluoride aqueous solutions with appropriate mixtures of 99.99% pure rare-earth oxides under hydrothermal conditions. Platelets of different compositions with thickness of about 1 mm were utilized for the OSL measurements (see Fig. 1). Besides, in order to evaluate the OSL efficiency of these materials, platelets of 0.5 at.% Pr^{3+} doped K_2YF_5 crystals synthesized with the same technique and Al_2O_3:C discs (Landauer Inc.) of 5 mm in diameter and 0.9 mm in thickness were used for comparison.

The samples were irradiated with a 10 mCi ophthalmic ^{90}Sr beta-source rendering a dose rate of 0.024 Gy min^{-1} at the sample position. For optical stimulation a Luxeon V Star green LED with maximum emission at 530 nm and a Luxeon III Star red LED with maximum emission at 627 nm were employed. Both of them were driven at 500 mA with a Newport 525B laser diode drive rendering an effective luminous flux of 128 and 56 lm at the sample position for the green and red LEDs, respectively. In each case the LED light was filtered by means of two 3 mm thick Schott OG530 long-pass filters before reaching the sample. Besides, two 3 mm thick Hoya B-390 band-pass filters were interposed between the sample and the light detector in order to get rid of the stimulation light by taking into account that the transmission window of the B-390 filter was in the spectral range from 320 to 500 nm and the maximum transmission occurred at 400 nm. Single-channel detection of the OSL signal was performed at room temperature (RT) by using a Hamamatsu H9319 photon counting head having sensitivity between 300 and 850 nm. For all measurements both irradiation and stimulation were applied to the same face of the sample from which the emitted light was detected.

In the present work the RL spectra of the investigated samples were measured by means of an Acton Research SP-2155 0.15 m monochromator featuring the above mentioned H9319 photon counting head as detector. The sample was placed at the entrance slit and back-irradiated by means of the ^{90}Sr source, which was situated 1 cm away from the sample. Both, the entrance and the exit slits were set to a width of 1 mm during the measurements rendering a resolution of 5 nm.

A Harshaw-Bicron 3500 TL reader was used for recording the TL emission of the investigated samples from RT up to 648 K with a constant heating rate of 1.0 K s^{-1}. Annealing of the samples at 648 K for 1 min was also performed immediately after recording the TL glow curve in order to empty completely the filled traps.

3. Results and discussion

Knowing the OSL spectra is crucial to determine the optimal combination of optical filters in order to maximize the collection of emitted light and prevent the stimulation light from reaching the light detector. Since the OSL emission is not stationary, obtaining its spectrum is not easy without resorting to multichannel highly sensitive detectors. However, it is expectable that the luminescence centers involved in OSL are the same participating in the radioluminescence (RL) process. For this reason, a first estimate of the OSL spectrum could be obtained by recording the spectrum of the light emitted by a sample during the RL experiment.

In Fig. 2 the spectra corresponding to the RL emission of the investigated compounds are depicted. As expected, Al_2O_3:C has a broad emission band centered at 420 nm [17]. On the other hand, K_2YF_5:Pr^{3+} crystals show two intense bands centered at 480 and 495 nm and a weak band extending from 585 up to 615 nm. In principle, bands at 480 and 495 nm could be assigned to the inter-Stark $^3P_0-^3H_4$ transitions of the Pr^{3+} cation in this host. In turn, the broad band emission could be related to $^1D_2-^3H_4$ transitions, which actually consist of several narrow bands corresponding to the different Stark levels involved in the radiative process. Although the position of the mentioned f–f transitions of Pr^{3+} is not expected to be strongly affected by the host due to outer 5s and 5p shielding, small shiftings could be possible depending on the actual crystal environment [18].

As to the fluorides singly doped with Tb^{3+} and doubly doped with Tb^{3+} and Ce^{3+} or Tb^{3+} and Dy^{3+}, they present several narrow bands at 380, 415, 435, 488, 540, 580 and 622 nm with different relative intensity depending on the Tb^{3+} concentration and the kind of the second doping ion. All of these bands can be attributed to characteristic Tb^{3+} transitions, namely, $^5D_3-^7F_j$ with $j=6$, 5, 4 and $^5D_4-^7F_j$ with $j=6$, 5, 4, 3, respectively [16]. As can be seen in Fig. 2, emission bands corresponding to transitions $^5D_3-^7F_j$ have relatively strong intensities only in K_2YF_5:1 at.% Tb^{3+}. The emission bands corresponding to transitions $^5D_4-^7F_j$ have similar intensities in all of the fluorides containing Tb^{3+} ions. The high Tb^{3+} concentration in K_2YF_5:10 at.% Tb^{3+} and K_2YF_5:10 at.% Tb^{3+}, 5 at.% Ce^{3+} could be responsible for the absence of $^5D_3-^7F_j$ emission bands in these compounds due to

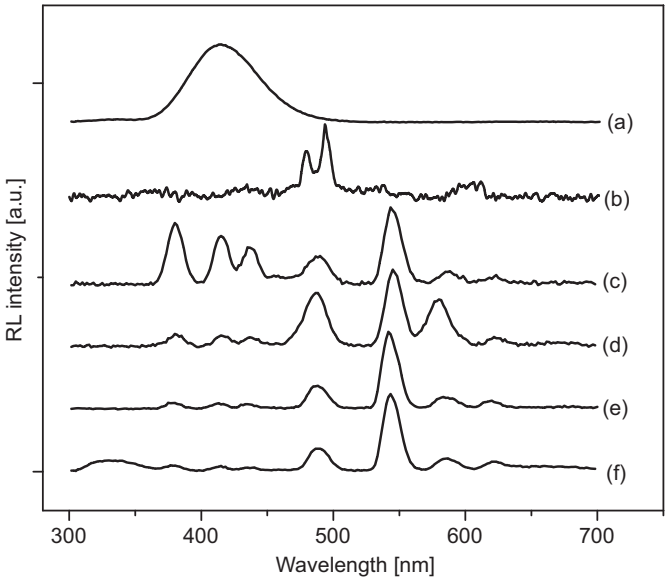

Fig. 2. RL spectra of (a) Al_2O_3:C, (b) K_2YF_5:0.5 at.% Pr^{3+}, (c) K_2YF_5:1 at.% Tb^{3+}, (d) K_2YF_5:1 at.% Tb^{3+}, 2 at.% Dy^{3+}, (e) K_2YF_5:10 at.% Tb^{3+} and (f) K_2YF_5:10 at.% Tb^{3+}, 5 at.% Ce^{3+}.

cross-relaxation among Tb^{3+} ions [17]. By the way, the weak broad band at 320 nm could be attributed to $d \rightarrow f$ Ce^{3+} transitions [12] by taking into account that most part of excited state Ce^{3+} energy is transferred to Tb^{3+} ions at these concentrations of Tb^{3+} and Ce^{3+}.

On the other hand, in K_2YF_5:1 at.% Tb^{3+}, 2 at.% Dy^{3+}, the $^5D_3 - ^7F_j$ emission bands have weak intensities as in the case of K_2YF_5:10 at.% Tb^{3+} and in contrast to K_2YF_5:1 at.% Tb^{3+}. Also there are no emission bands which could be attributed to the Dy^{3+} radiative transitions but there is more efficient luminescence due to the $^5D_4 - ^7F_j$ transitions in K_2YF_5:1 at.% Tb^{3+}, 2 at.% Dy^{3+} than in other studied compositions. Accordingly, one can assume that there is energy transfer from Dy^{3+} ions to Tb^{3+} ions due to, for example, resonance between the $^4F_{9/2}$ Dy^{3+} and the $^5D_4$ Tb^{3+} energy levels. In addition, the energy gap between the $^5D_3$ and $^5D_4$ levels in Tb^{3+} matches with the gap between the ground $^6H_{15/2}$ and the second excited $^6H_{11/2}$ states in Dy^{3+}. Thus, cross-relaxation between Dy^{3+} and Tb^{3+} are possible and this cross-relaxation process produces the population of the $^5D_4$ level at the expense of the $^5D_3$ level, thereby resulting in strong luminescence from the $^5D_4$ level [21].

The decision to use the Hoya B-390 filter with a center wavelength of 390 nm and FWHM of 125 nm as emission filters in our experimental setup for investigation OSL is based on the spectra shown in Fig. 2 and the available stimulation systems already mentioned in the previous section. In fact, the Hoya B-390 filters permit to collect almost all of the light emitted by Al_2O_3:C and the part of the luminescence output corresponding to the $^5D_3 - ^7F_j$ emission bands from the Tb^{3+} doped samples investigated in this work. However, it should be noted that the chosen filtering setup is not entirely consistent with the emission spectrum of K_2YF_5:Pr^{3+} and only a small portion of the luminescence output from this composition can be collected during OSL experiments.

Fig. 3 shows the OSL response of K_2YF_5 crystals containing Tb^{3+} ions and, as can be see, K_2YF_5 singly doped with 1 at.% Tb^{3+} has the highest OSL intensity. As mentioned, the filtering setup is in part responsible for this result in addition to the intrinsic efficiency of this composition. The effect of different stimulation wavelengths on the OSL output can be observed in Fig. 4, where the OSL responses stimulated either with red or green light for crystals of K_2YF_5:1 at.% Tb^{3+} irradiated with a dose of 0.24 Gy are depicted. It is apparent that OSL is more efficient when green

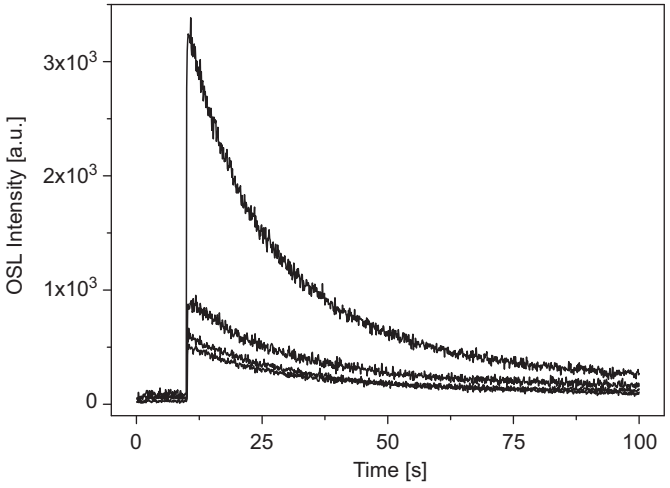

Fig. 3. OSL of K_2YF_5:1 at.% Tb^{3+}, K_2YF_5:10 at.% Tb^{3+}, K_2YF_5:10 at.% Tb^{3+}, 5 at.% Ce^{3+} and K_2YF_5:1 at.% Tb^{3+}, 2 at.% Dy^{3+}, from top to bottom, respectively. The samples were irradiated with a dose of 0.24 Gy and the OSL signal has been normalized to the sample weight.

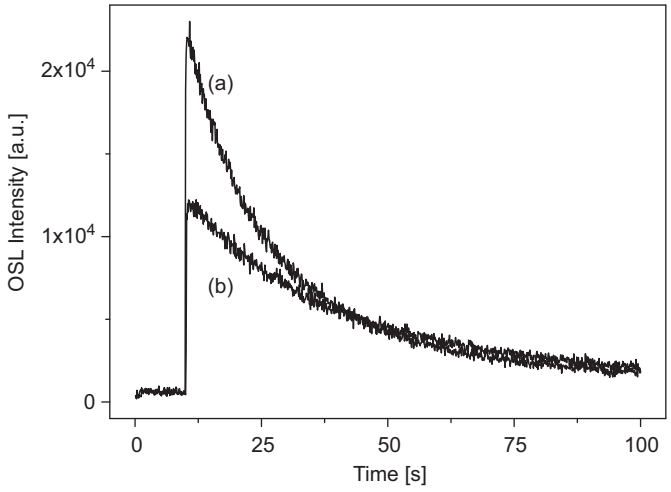

Fig. 4. OSL signal from K_2YF_5:1 at.% Tb^{3+} crystals stimulated with (a) green light and (b) red light exposure with a dose of 0.24 Gy.

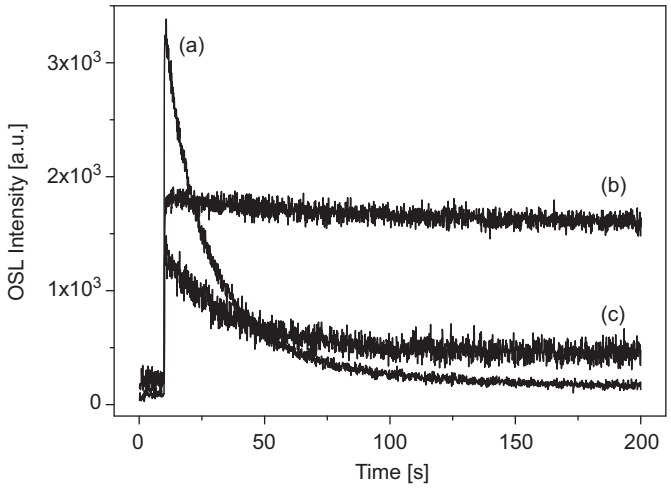

Fig. 5. OSL signal from (a) K_2YF_5:1 at.% Tb^{3+}, (b) Al_2O_3:C (multiplied by 10) and (c) K_2YF_5:0.5 at.% at Pr^{3+} (multiplied by 10). The samples were irradiated with a dose of 0.24 Gy and the OSL signals were normalized to the sample weight.

stimulation is employed. The same results have been observed for others investigated fluoride compositions. In what follows, all the OSL measurements have been performed with the green LED as stimulation source.

In order to have a practical estimate of the OSL efficiency for K_2YF_5:1 at.% Tb^{3+} as a dosimeter, its OSL response has been compared to that of a commercial Al_2O_3:C chip and a crystal K_2YF_5:Pr^{3+} plate. As can be seen in Fig. 5, the maximum OSL intensity of K_2YF_5:1 at.% Tb^{3+} is higher by an order of magnitude or more than those of Al_2O_3:C and K_2YF_5:Pr^{3+}. On the other hand, the OSL signal of K_2YF_5:1 at.% Tb^{3+} decays much faster than of Al_2O_3:C and fades out completely after stimulation for 200 s. This result implies, from the viewpoint of the application of K_2YF_5:1 at.% Tb^{3+} (1 at.%) as OSL dosimeter, that the OSL readout empties most of the trapped charges in this composition so that no any additional optical bleaching process is necessary before reutilization. The dose response of K_2YF_5:1 at.% Tb^{3+} has also been preliminary studied. Fig. 6 shows the OSL curves from K_2YF_5:1 at.% Tb^{3+} after irradiation to different doses ranging from 0.024 up to 2.4 Gy. As can be seen, a good linearity is observed in the studied dose range.

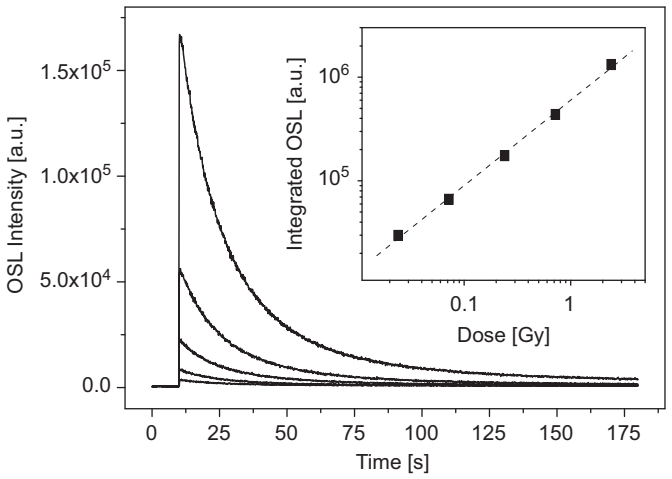

Fig. 6. OSL signal from K_2YF_5:1 at.% Tb^{3+} for different irradiation doses, namely 2.40, 0.72, 0.24, 0.072 and 0.024 Gy, from top to bottom one after another. In the inset: dose–response curve of the integrated OSL signal under green stimulation for K_2YF_5:1 at.% Tb^{3+} exposed to different beta doses.

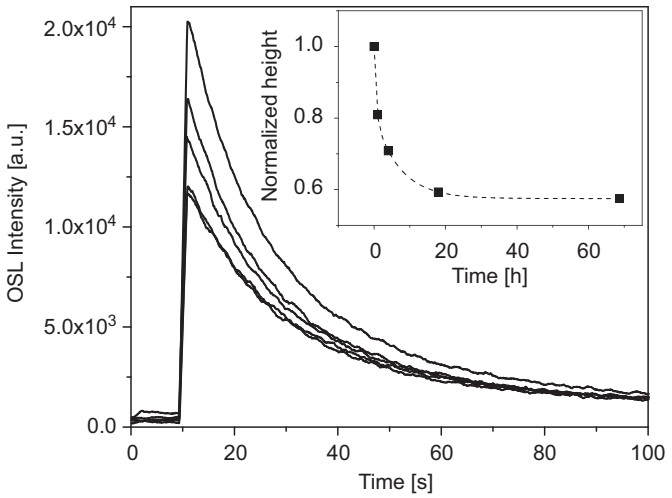

Fig. 7. OSL signal from K_2YF_5:1 at.% Tb^{3+} measured after different storage times, namely 0, 1, 4, 18 and 69 h, from top to bottom one after another. In the inset: the normalized height of the OSL signal as a function of the storage time.

The fading of the OSL signal of K_2YF_5:1 at.% Tb^{3+} for different storing times in dark at RT after irradiation has been investigated. As can be seen in Fig. 7 the maximum intensity of the OSL signal decreases by approximately 40% during the first 20 h of storing and no additional fading is observed after this time period. This partial emptying of OSL traps could be related to shallow traps present in the material as fabrication defects. In order to evaluate this possibility, the TL glow curve of K_2YF_5:1 at.% Tb^{3+} has been measured after 18 h of storage in dark at RT and this curve has been compared with the glow curve measured immediately after irradiation (see Fig. 8). It is apparent from the figure that only the lowest temperature peak in the K_2YF_5:1 at.% Tb^{3+} glow curve measured promptly after irradiation disappears during storage, which in principle confirms the previous assertion. From the viewpoint of dosimetry, the negative effect of the observed OSL fading could be avoided by annealing the K_2YF_5:1 at.% Tb^{3+} samples before the OSL readout. In fact, if a preheat treatment at 80 °C during 10 s is performed on the irradiated samples, no fading in the TL and the OSL signals is observed.

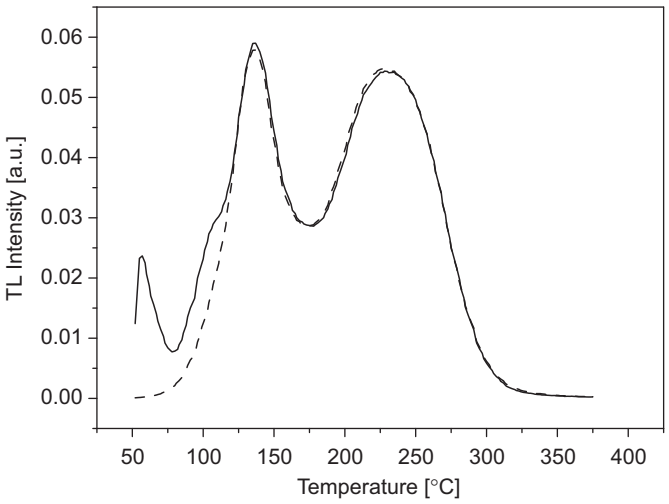

Fig. 8. TL glow curve from irradiated K_2YF_5:1 at.% Tb^{3+} before (solid line) and after the 18 h period of storage (dashed line).

4. Conclusions

The OSL properties of K_2YF_5 crystals singly doped with different concentrations of Tb^{3+} ions and doubly doped with Tb^{3+} and Ce^{3+} or Tb^{3+} and Dy^{3+} have been investigated for the first time. K_2YF_5:1 at.% Tb^{3+} has been found to be the most efficient OSL detector among the studied compositions and its efficiency is similar to that of Al_2O_3:C. The K_2YF_5:1 at.% Tb^{3+} detector presents a linear response in the studied dose range from 0.024 to 2.4 Gy and no fading is observed if irradiated samples are preheated at 80 °C. The obtained results show that the use of this material in radiation dosimetry is feasible.

Acknowledgments

This work was partially supported by grant PICT Red Nr. 1907 from Agencia Nacional de Promoción Científica y Tecnológica (ANPCyT, Argentina), Grant no. 636/QD-KHCNVN from the Vietnam Academy of Science and Technology (VAST), Grants 10-02-91167 and 10-03-90305 from the Russian Foundation for Basic Research (RFBR). J. Marcazzó thanks to DGAPA-UNAM (Mexico) for supporting his postdoctoral position.

References

[1] S.W.S. McKeever, Nucl. Instr. Meth. Phys. Res. B 184 (2001) 29.
[2] C.A. Perks, G. Le Roy, B. Prugnaud, Radiat. Prot. Dosim. 125 (2007) 220.
[3] M. Sommer, R. Freudenberg, J. Henniger, Radiat. Meas. 42 (2007) 617.
[4] M. Sommer, A. Jahn, J. Henniger, Radiat. Meas. 43 (2008) 353.
[5] P. Dorenbos, R. Visser, C.W.E. Van Eijk, IEEE Trans. Nucl. Sci. 40 (1993) 388.
[6] D.R. Schaart, P. Dorenbos, C.W.E. van Eijk, R. Visser, C. Pedrini, B. Moine, N.M. Khaidukov, J. Phys. Condens. Matter 7 (1995) 3063.
[7] N. Kristianpoller, D. Weiss, R. Chen, N. Nariyama, N.M. Khaidukov, Radiat. Prot. Dosim. 100 (2002) 207.
[8] J. Marcazzó, M. Santiago, E. Caselli, N. Nariyama, N.M. Khaidukov, Opt. Mater. 26 (2004) 65.
[9] D. McLean, J. Varas, N. Khaidukov, Radiat. Phys. Chem. 71 (2004) 995.
[10] L.O. Faria, D. Lo, H.W. Kui, N.M. Khaidukov, M.S. Nogueira, Radiat. Prot. Dosim. 112 (2004) 435.
[11] E. Caselli, P. Molina, M. Santiago, F. Ortega, N. Khaidukov, F. Spano, C. Furetta, Biomed. Tech. 50 (2005) 1301.
[12] H.W. Kui, D. Lo, Y.C. Tsang, N.M. Khaidukov, V.N. Makhov, J. Lumin. 117 (2006) 29.
[13] E.C. Silva, N.M. Khaidukov, M.S. Nogueira, L.O. Faria, Radiat. Meas. 42 (2007) 311.
[14] J. Marcazzó, M. Santiago, C. D'Angelo, C. Furetta, E. Caselli, Nucl. Instr. Meth. Phys. Res. B 268 (2010) 183.
[15] J. Marcazzó, N.M. Khaidukov, E. Caselli, C. Dangelo, M. Santiago, Phys. Status Solidi (a) 206 (2009) 2593.

[16] A.J.J. Bos, M. Prokic, J.C. Brouwer, Radiat. Prot. Dosim. 119 (2006) 130.
[17] J. Marcazzó, J. Henniger, N.M. Khaidukov, V.N. Makhov, E. Caselli, M. Santiago, J. Phys. D Appl. Phys. 40 (2007) 5055.
[18] J. Isasi-Marín, M. Pérez-Estébanez, C. Díaz-Guerra, J.F. Castillo, V. Correcher, M.R. Cuervo-Rodríguez, J. Phys. D Appl. Phys. 42 (2009) 075418.
[19] J.C. Mittani, M. Prokic, E.G. Yukihara, Radiat. Meas. 43 (2008) 323.
[20] M.A. Dubinskii, N.M. Khaidukov, I.G. Garipov, L.N. Dem'yanets, A.K. Naumov, V.V. Semashko, V.A. Malyusov, J. Mod. Opt. 37 (1990) 1355.
[21] A. Santana-Alonso, A.C. Yanes, J. Mendez-Ramos, J. del-Castillo, V.D. Rodriguez, Opt. Mater. 33 (2011) 587.